



HAL
open science

Results from single event effect tests with MIMOSIS-1

B Arnoldi-Meadows, J Andary, O Artz, J Baudot, G Bertolone, A Besson, N Bialas, R Bugiel, G Claus, C Colledani, et al.

► **To cite this version:**

B Arnoldi-Meadows, J Andary, O Artz, J Baudot, G Bertolone, et al.. Results from single event effect tests with MIMOSIS-1. *Journal of Instrumentation*, 2023, 18 (04), pp.C04002. 10.1088/1748-0221/18/04/C04002 . hal-04060226

HAL Id: hal-04060226

<https://hal.science/hal-04060226>

Submitted on 27 Nov 2023

HAL is a multi-disciplinary open access archive for the deposit and dissemination of scientific research documents, whether they are published or not. The documents may come from teaching and research institutions in France or abroad, or from public or private research centers.

L'archive ouverte pluridisciplinaire **HAL**, est destinée au dépôt et à la diffusion de documents scientifiques de niveau recherche, publiés ou non, émanant des établissements d'enseignement et de recherche français ou étrangers, des laboratoires publics ou privés.



Distributed under a Creative Commons Attribution 4.0 International License

PAPER • OPEN ACCESS

Results from single event effect tests with MIMOSIS-1

To cite this article: B. Arnoldi-Meadows *et al* 2023 *JINST* **18** C04002

View the [article online](#) for updates and enhancements.

You may also like

- [Resolution improvement of dipole source localization for artificial lateral lines based on multiple signal classification](#)
Mingjiang Ji, Yong Zhang, Xiande Zheng *et al.*
- [The compressed baryonic matter \(CBM\) experiment at FAIR—physics, status and prospects](#)
Kshitij Agarwal and for the CBM Collaboration
- [Tolerance of the MIMOSIS-1 CMOS Monolithic Active Pixel Sensor to ionizing radiation](#)
H. Darwish, J. Andary, B. Arnoldi-Meadows *et al.*

23RD INTERNATIONAL WORKSHOP ON RADIATION IMAGING DETECTORS
26–30 JUNE 2022
RIVA DEL GARDA, ITALY

Results from single event effect tests with MIMOSIS-1

B. Arnoldi-Meadows,^{a,*} J. Andary,^a O. Artz,^a J. Baudot,^b G. Bertolone,^b A. Besson,^b
N. Bialas,^a R. Bugiel,^b G. Claus,^b C. Colledani,^b H. Darwish,^{a,b,c} M. Deveaux,^{a,c}
A. Dorokhov,^b G. Dozière,^b Z. El Bitar,^b I. Fröhlich,^{a,c} M. Goffe,^b F. Hebermehl,^a
A. Himmi,^b C. Hu-Guo,^b K. Jaaskelainen,^b O. Keller,^f M. Koziel,^a F. Matejcek,^a
J. Michel,^a F. Morel,^b C. Müntz,^a H. Pham,^b C. J. Schmidt,^c S. Schreiber,^a M. Specht,^b
D. Spicker,^a J. Stroth,^{a,c,d} I. Valin,^b K.-O. Voss,^c R. Weirich,^a Y. Zhao^b and M. Winter^e

^aInstitut für Kernphysik, Goethe-Universität Frankfurt,

Max-von-Laue-Straße 1, 60438 Frankfurt am Main, Germany

^bUniversité de Strasbourg, CNRS, IPHC UMR 7178, 67037 Strasbourg Cedex 2, France

^cGSI Helmholtzzentrum für Schwerionenforschung GmbH,

Planckstraße 1, 64291 Darmstadt, Germany

^dHelmholtz Forschungsakademie Hessen für FAIR, Max-von-Laue-Straße 12,

60438 Frankfurt am Main, Germany

^eUniversité Paris-Saclay, CNRS/IN2P3, IJCLab, 91405 Orsay, France

^fFacility for Antiproton and Ion Research GmbH, Planckstraße 1, 64291 Darmstadt, Germany

E-mail: b.arnoldi-meadows@gsi.de

ABSTRACT: Being installed as close as 5.5 mm to the beam axis, the Micro Vertex Detector (MVD) of the CBM experiment will be exposed to a sizable flow of heavy beam ions and nuclear fragments. The CMOS Monolithic Active Pixel Sensor for the MVD, MIMOSIS, must resist the related heavy ion impacts without permanent damage or frequent interrupt of operation as caused by single event effects (SEE). We motivate the requirements on the sensor and introduce our concept for protecting the device against SEEs. Moreover, we report the results of a related test campaign carried out with the first full size sensor prototype, MIMOSIS-1, and different heavy ion beams at GSI.

KEYWORDS: Particle tracking detectors; Radiation-hard detectors

*Corresponding author.

Contents

1	Introduction	1
1.1	The MIMOSIS-1 sensor	1
1.2	Requirements on the heavy ion tolerance of the MVD	2
2	Experimental setup and findings	3
2.1	Detection strategies for SEE	3
2.2	Pb beam	4
2.3	Xe beam	5
2.4	M3 beam	6
3	Discussion, conclusions and open issues	7

1 Introduction

Thanks to their high granularity, low material budget, and moderate power consumption, CMOS Monolithic Active Pixel Sensors (MAPS) are well-suited to be used in high-precision vertexing and tracking detectors in heavy ion experiments. The CBM experiment at FAIR, a next-generation fixed-target heavy ion experiment, will feature a four-plane Micro Vertex Detector (MVD) based on MAPS technology. The MVD is currently being developed to run in this context in target vacuum, placing the MIMOSIS sensor in close proximity to the target and the beam axis (down to 5 cm and ~ 5.5 mm, respectively).

MIMOSIS will be equipped with a pixel matrix of 1024 columns of each 504 pixels. The pixel size amounts to $27 \times 30 \mu\text{m}^2$. The sensor will be built in the TowerJazz 180 nm CMOS image sensor process. The pixels will incorporate a full amplifier-shaper-discriminator chain, which samples-and-holds the signal of impinging particles during its frame time of 5 μs . Hereafter, the hit information will be forwarded to a dual port memory cell and then read out via a priority encoder shared by two columns. The data will be transported via few data concentration buffers toward an elastic buffer which can receive data fluxes corresponding to hit data rates of up to $\sim 80 \text{ MHz/cm}^2$. The data buffer will then send a data stream of up to 2.4 Gbps (corresponding to hit data rates $\sim 20 \text{ MHz/cm}^2$) out of the sensor. The purpose of the elastic buffer consists in accommodating data bursts exceeding the average particle rate by a factor of three for up to 50 μs . This feature is designed to mitigate effects of beam intensity fluctuations expected at SIS100. Further details on the concept of MIMOSIS are discussed in [1–3].

1.1 The MIMOSIS-1 sensor

MIMOSIS-1 is the first full size prototype of MIMOSIS. Most functionalities of the final sensor (and all of the features mentioned above) have already been realized in MIMOSIS-1.

The prototype sensors have been extensively characterized to study sensing element design options, the digital readout and to confirm the targeted radiation tolerance. Results of in-beam performance studies of MIMOSIS-1 sensors before and after irradiation with ionizing radiation are reported in [1, 2].

The studies presented in this report relate to the testing of both digital front end and the analog sensing elements with regard to their hardness against Single Event Effects (SEE). Single event effects occur when ionizing radiation (e.g. heavy ions) impinges semiconductor detector material and generates a sizable number of minority charge carriers, which impact the functioning of on-chip microelectronics. Two particularly relevant SEE are so-called bitflips (also often SEU) and latch-ups (also often SEL, in this text also LU). Bitflips are typically soft errors that can be recovered by reprogramming the affected memory cells. The term latch-up denotes a meta-stable short circuit, which stems from parasitic thyristors being switched into their conductive state by the minority charge carriers. This may thermally destroy the device unless the thyristors are reset to their non-conductive state by means of a power cycle.

MIMOSIS-1 is protected against single event latch-ups by using suited design rules, e.g. by placing structures to evacuate the injected minority charge carriers before they can open conductive channels. Moreover, all steering registers are protected against bitflips by an error correction relying on Hamming encoding. This concept is suited to automatically recover flips of one individual bit in each steering register. As will be detailed below, this feature is found not to work properly in MIMOSIS-1 due to a mistake in its implementation. No protection for the hit data registers are foreseen as a smaller amount of bit errors in the data is considered acceptable. Still, selected important messages (e.g. the start of a novel integration period) are redundant to keep the synchronization between sensor and DAQ system also in the event of bit errors. The future MIMOSIS-2 will host further protective features as a triple redundancy of the clock and the most important state machines. Those features were intentionally not (yet) implemented in MIMOSIS-1.

1.2 Requirements on the heavy ion tolerance of the MVD

The MVD will be exposed to heavy ions from at least three sources: the beam halo, slow target fragments, and direct beam impacts caused by problems with the beam steering magnets. The beam halo is dominated by beam ions which are traveling significantly aside the beam center due to the limitations of the focusing system of the synchrotron. In the case of CBM, this halo will be reduced by means of a dedicated collimator system located upstream the last beam dipole magnets. The specification of the MVD require that the sensors should be exposed to a maximum continuous rate of 1 kHz/cm^2 beam ions. This number is motivated by the integrated radiation dose created by the heavy ions and forms a requirement to the quality of the beam reaching CBM [3]. Beam halo ions are relativistic heavy ions, typically creating a linear energy transfer (LET) of $\sim 10 \text{ MeV cm}^2/\text{mg}$.

When the MVD is installed, CBM will operate with heavy ion beams of a beam intensity of 10 MHz. It is anticipated that this beam will be a constant profile beam focused to a radius of 1 mm [3]. In case the beam hits the detector due to a beam steering issue, it will create a local ion flux

of ~ 300 MHz/cm². The sensors have to tolerate this flux without permanent damage until a beam abort is triggered. It is considered that this beam abort system will stop the beam in the order of 100 μ s [3].

The impact of target fragments was studied by means of a Monte Carlo simulation relying on the CbmRoot simulation framework [4] and its associated FairIonGenerator class, which computes the properties of nuclear fragments created in heavy ion collisions. The simulated particles were propagated through a realistic detector model with the GEANT4 transport engine [5]. The impact position of the ions in the detector as well as their momenta and energies were recorded. It was found that many ions penetrate the 5 cm long distance between the target and the first sensor despite being deflected by the 0.3–1 T magnetic field present in this gap. The necessary momentum is generated rather by the high rest mass of the ions than by a high velocity, thus the kinetic energies of the ions remain as low as some A MeV. Therefore, a significant number of particles are absorbed in the ~ 10 μ m thick entrance window of the top illuminated sensors. This holds true in particular for ions of higher charge which are found to be particularly slow. Ignoring ions which are absorbed in the entrance window, it is found that the transistors of the sensors may be exposed to LETs of $\gtrsim 35$ MeV cm²/mg. This value represents a lower limit as rare fragments of higher LETs might have been overlooked due to limited statistics of the simulation. More information on the simulation is found in [6].

We require that the most exposed sensor in CBM should operate for more than one hour without a need for an intervention (reprogramming, power cycle) recovering the consequences of a SEE. Assuming a constant beam halo of 1 kHz/cm², this translates to a maximum tolerable SEE cross-section of $\sim 3 \times 10^{-7}$ cm² per MIMOSIS sensor for regular beam ions. Moreover, the sensors should tolerate occasional impacts of ions creating an LET of > 35 MeV cm²/mg as well as an impact of a primary beam with a flux of ~ 300 MHz/cm² for a duration safely above 100 μ s without lasting damage.

2 Experimental setup and findings

2.1 Detection strategies for SEE

The measurement program reported consisted in three consecutive beam times at different heavy ion beam lines at the GSI facility in Darmstadt, Germany. The initial focus of the program was laid on identifying single-event latch-ups (LUs). In accordance with earlier reports [7, 8], we intended to identify those LUs by the related over-currents. By doing so, we assumed implicitly the MIMOSIS sensor to show an approximately constant power consumption during its operation. As discussed in detail below, this assumption came out not to be fully valid. Consequently, the general experimental strategy detailed below was modified during the program in response to unexpected observations, as will be described in the sections 2.3 and 2.4.

The sensors under test were bonded on a dedicated proximity board which was derived from the regular proximity board used for testing the sensor. However, all active — and thus potentially radiation soft — components of the board were removed knowing it would be exposed to sizable radiation doses. By doing so, the access to the data output of the sensors was sacrificed in exchange for radiation tolerance. Moreover, the analog and digital power was provided to the sensor by a

dedicated, so-called latch-up protection board. This board biased the sensors via shunt resistors used in combination with a discriminator to automatically cut the power once over currents as caused by a LU were detected. The status of the board and two voltages proportional to the analog and digital current respectively were sent as an analog signal via the wires in a 30–90 m long RJ45 cable to an operator board located in the counting house. This operator board contained, among others, switches to reset the power of the sensor and allowed for monitoring the mentioned voltages by means of an oscilloscope.

The simple initial measurement strategy consisted in illuminating the sensor with heavy ions and manually counting the number of power cuts caused by the biasing currents exceeding the threshold. Moreover, we were manually reading back the content of slow control registers by means of our slow control software in order to spot possible bitflips by manual comparison. This simplistic approach reflected the existing option to adapt the beam intensity to obtain a manageable SEE rate, and the assumption that no, or only very few bitflips were to be expected.

2.2 Pb beam

Our first test was mostly intended to validate our test strategy. The MIMOSIS-1 sensor was mounted in front of the beam dump of the mCBM [9] beam line located at the SIS18 synchrotron at GSI. The sensors were exposed to an $E_{\text{kin}} = 1.05A$ GeV Pb beam creating an estimated LET of $12 \text{ MeV cm}^2/\text{mg}$, which was calculated under the assumption that the ions are fully stripped shortly after impinging the sensor material. The sensor was exposed to about 3×10^9 ions within few hours. The related dosimetry gave rise to a sizable source of uncertainty as it relied solely on beam instrumentation, which was not designed or calibrated for this purpose. Besides knowing that the sensor was most likely not uniformly illuminated, we anticipate that the total number of ions is determined with an uncertainty of a factor three at best.

During the experiment, the thresholds of the sensor were put to a minimum value. This was done in order to saturate the data buses and therefore to suppress power fluctuations as caused by varying data load. Despite this step should force a constant power consumption of the digital current, we observed SEE reducing this current. In coincidence with this observation, we noticed that values stored in the steering registers of the sensor had changed as would be expected in the case of non-corrected single bitflips. We concluded that the state of the sensor changed due to bitflips, which created a change of its power consumption. A total of 50 SEE events were identified based on a change on current drawn or a triggered overcurrent protection. During a dedicated test phase, where we logged all registers when we saw the current drawn fluctuating. From this, we identified about a 25% larger amount of bitflips. As this was only possible if the overcurrent protection was not triggered, we estimate that the true number of SEE is about 50% higher, yielding ~ 75 SEE.

The unexpected observation of those single bitflips turned out as the most important result of this first test. By following it up, the sensor designers spotted a bug in the implementation of the Hamming code protection of the steering registers, which will be fixed in follow-up prototype MIMOSIS-2. As single bitflips show also the potential to raise the power consumption of the sensor above threshold in the absence of an LU, only a combined SEE cross-section could be estimated. As suggested by the JEDEC 57A standard [10], this cross-section (per sensor!) is defined in this

work as

$$\sigma = \frac{N_{\text{SEE}}}{\phi} \quad (2.1)$$

with N_{SEE} the number of single event effects observed.

$$\phi = \frac{N_{\text{ion}}}{A} \quad (2.2)$$

is the ion fluence defined as the number of ions impinging the sensor surface¹ of $A = 5.3 \text{ cm}^2$.

Assuming naively that the $\sim 3 \times 10^9$ ions were impinging the sensor with homogeneous distribution, one obtains a coarse result for this cross-section, which is $\sigma = \mathcal{O}(10^{-7} \text{ cm}^2)$ per sensor. As, however, the most vulnerable structure of the sensors (the DACs, see below), were likely at the border or outside the beam spot, this number should be used with caution.

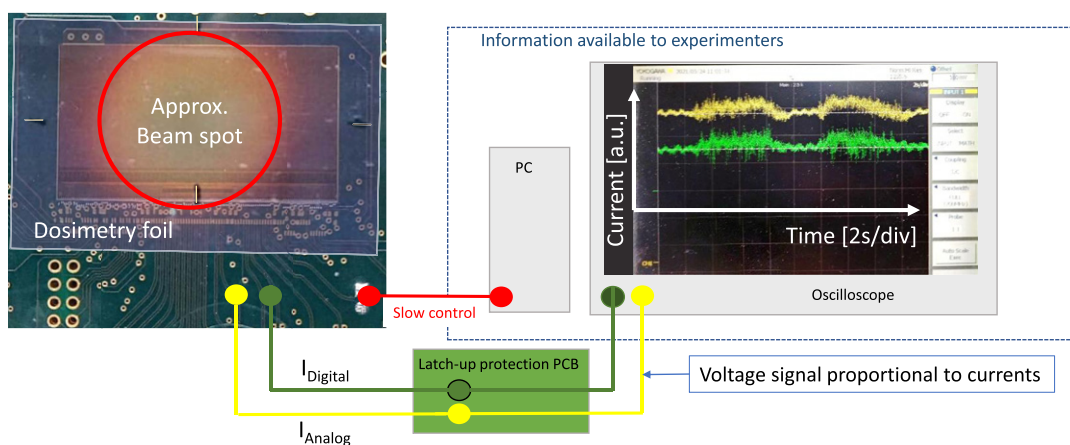


Figure 1. Experimental setup as used in the beam test with the relativistic Xe beam. The beam spot as measured with the dosimetry foil in the absence of a target is shown.

2.3 Xe beam

The consecutive beam test was carried out with an $E_{\text{kin}} = 1.3 \text{ A GeV}$ Xe beam again at the mCBM beam line with an estimated LET of $5 \text{ MeV cm}^2/\text{mg}$ for fully stripped ions. While the setup is in general the same as in subsection 2.2, we improved our procedures by positioning a dosimetry foil on top of the sensor. Despite saturating, this foil gave an estimate on the size of the beam spot on the sensor (see figure 1). Moreover, we modified our procedure for spotting LUs. Encouraged by the robustness of the sensor observed during the previous test, we disabled the automatic power cycling and monitored the sensor currents visually on the oscilloscope. Once an excess current was observed, we tried to recover this state by reprogramming the status registers. In case of success, we rated the incident as bitflip. In case the excess current persisted, we performed a manual power cycling and rated the incidence as latch-up. By doing so, we revised our previous assumption that the power consumption of the sensor is constant in the absence of a latch-up. However, we assumed that bitflips could be in general recovered by reprogramming the sensor. This came out

¹ Defined as the surface of the full chip including the pixel matrix and the supporting on-chip electronics.

to be incomplete as the erroneous Hamming encoding system can fall into a state preventing the registers from being reprogrammed without hard reset. This fact was still unknown at the time of the experiment.

Still, the procedure allowed for a first time to obtain a rough separate estimate on the cross-sections for bitflips and LUs. We obtained $\sigma = O(10^{-8} \text{ cm}^2)$ per sensor for bitflips and $\sigma = O(10^{-9} \text{ cm}^2)$ for LUs. Remarkably, the LU cross-section is found to be small as compared to the bitflip cross-section, which likely stems from the bug in the Hamming encoding.

2.4 M3 beam

To overcome a number of the experimental weaknesses of the previous tests, a consecutive beam time was conducted at the M3 beam of the GSI UNILAC. This facility is equipped with a precise and calibrated dosimetry system, which eliminated the related major uncertainties. Moreover, the beam line provided $\sim 4.8 \text{ A}$ MeV Ca ions, which penetrate silicon and aluminum only into a depth of few $10 \text{ }\mu\text{m}$. This lower beam energy and penetration power allowed to stop the beam by means of a $600 \text{ }\mu\text{m}$ thick aluminium mask. To exploit this feature, we defined regions of interest on the sensor, which were chosen to include all potentially vulnerable structures of the design and thus to represent the full sensor. Over all, $\sim 60\%$ of the total sensor surface was illuminated. The remaining surface was either empty or covered with repetitive structures found also on the illuminated surface. Masking allowed to isolate the response of the individual regions of interest of the sensor and thus to identify vulnerable structures. Two complementary aluminium masks were prepared by means of a precise laser cutter and aligned to the sensor structures of interest by means of an optical microscope.² Each mask contained multiple openings, which were temporarily closed by means of aluminium tape. Figure 2(a) shows a mask together with the related MIMOSIS-1 sensor.

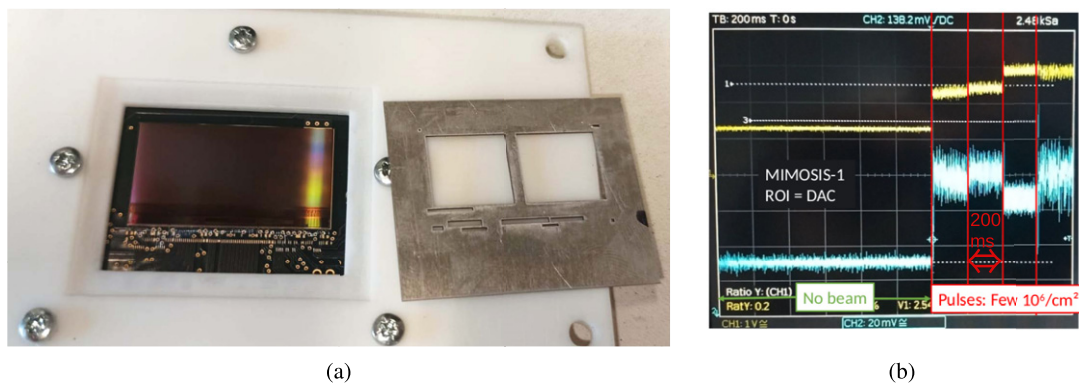


Figure 2. (a) Mask made from aluminum that was placed in front of sensor during tests described in subsection 2.4. Cutouts correspond to general regions of interest. Individual regions were selected by glueing aluminium tape in front of cutouts. (b) Screenshot of the oscilloscope during tests described in subsection 2.4 when the beam was illuminating MIMOSIS-1's DACs.

²The use of two pairs of masks and sensors turned out to be of advantage as the aluminium was moderately activated during the illumination. Thanks to the short half life of the isotopes created, one mask could cool down and hereafter be modified in a safe way while the other was used in beam.

To verify that the ions would penetrate the about $10\ \mu\text{m}$ thick entrance window of the sensor, which is formed from its metal lines and the surrounding SiO_2 , we simulated the interaction of the beam ions and the entrance window with the SRIM simulation package [11]. The simulation accounted for the energy loss of the ions in the Kapton foil separating the beam vacuum from the laboratory air and the $<5\ \text{mm}$ thin air gap between the sensor and this foil, which decelerates the ions to about $2.8A\ \text{MeV}$ before they reach the sensor itself. We conclude that the beam ions safely reach the vulnerable structures, which are identified as the region of P- and N-wells forming the transistors, and proceed further into the epitaxial layer. Moreover, the simulation confirmed that a LET of $20\ \text{MeV cm}^2/\text{mg}$ was deposited by fully stripped ions into the vulnerable structures.

The regions of interest were illuminated with a beam intensity of $\sim 10^7\ \text{Hz/cm}^2$ up to a minimum integrated fluence of $\phi = 3 \times 10^{10}$ ions per cm^2 corresponding to $\phi = 1.6 \times 10^{11}$ per sensor. As the beam has a 2.5% duty cycle (5 pulses of each 5 ms per second), the ion flux during the pulses amounted $\sim 400\ \text{MHz/cm}^2$. Therefore, the illumination occurred at the ion flux expected for the CBM beam loss scenario for a much longer period of time than defined as a requirement, which demonstrated in passing the robustness of the sensors to such a beam loss scenario.

In contrast to our expectations, not a single LU was observed during the full test campaign at the M3 beam line. This holds independently of the back bias chosen, which was varied between $-1\ \text{V}$ and $-3\ \text{V}$. In the likely scenario that the regions of interest are representative for the full chip, this sets an upper limit of

$$\sigma < \frac{3.7 \cdot 5.3\ \text{cm}^2}{1.6 \times 10^{11}\ \text{ions}} = 1.2 \times 10^{-10}\ \text{cm}^2 \quad (2.3)$$

per one given sensor to the latch-up cross-section. As recommended by [10], we set artificially $N_{\text{SEE}} = 3.7$ in order to obtain a 95% confidence that the true cross-section is below the number stated.

Instead of LUs, we observed a significant response to the ions once bombarding the DACS generating the steering voltages and currents of the sensor. As illustrated in the screenshot in figure 2(b), the power consumption of the sensor was modified essentially during each individual ion pulse hitting the DACS, which has been identified a signature of at least one bit flipping in cells of the DACS. Unfortunately, it was not possible to extract quantitative data on this effect as this would have required to dim the beam below the minimum sensitivity limit of the available dosimetry system.

Instead, additional tests were conducted at the GSI X0 micro-beam line, where a focused pencil beam ($\sim 500\ \text{nm FWHM}$) was used to scan memory cells. This data is currently under analysis.

3 Discussion, conclusions and open issues

Our measurement campaign provides relevant insights concerning both the methods for studying SEE in CMOS sensors and on the tolerance of our detector under test, the MIMOSIS-1 sensor. Concerning the measurement protocol, our initial approach of using the current consumption of the device under test as the sole indicator for LUs is found to be insufficient. This is as the power

consumption of the sensor may vary for other reasons including load variations of the internal data buses and modifications of its settings. A good test protocol as much as a LU protection system must distinguish those trivial power fluctuations from LU signatures. The experience made suggests to test the power consumption of the sensor during spill breaks and after confirming the validity of its steering parameters.

Accounting for the results of the M3 beam time, we consider that most, if not all, of the LU signatures observed in the previous beam times were caused by bitflips in the steering registers of the power regulators. The observed vulnerability of those steering registers was understood thanks to the reported measurement campaign and will be eliminated in the next prototype MIMOSIS-2.

Besides spotting this vulnerability, the measuring campaign at the M3 beam demonstrated that the LU cross-sections of MIMOSIS-1 satisfy the needs of the CBM experiment. Moreover, the prototype resisted to heavy ion flows as expected for the event of a direct beam impact into the CBM-MVD without observed damage. No quantitative statement on the cross-sections for bitflips is made and we discourage to interpret our intermediate results as such.

Overall, the results obtained demonstrates the robustness of the MIMOSIS architecture to direct heavy ion impacts. Remaining open questions concerning the robustness to bitflips will be addressed by follow-up experiments with the MIMOSIS-2 sensor, which will host improved protective measures.

Acknowledgments

This project has received funding from the European Union’s Horizon 2020 research and innovation programme under grant agreement No. 871072 (Eurizon), BMBF under Grant No. 05P21RFFC2, HFHF, HGS-HIRE, and Tangerine.

References

- [1] A. Dorokhov et al., *The MIMOSIS pixel sensor for the CBM micro-vertex detector and beyond, Proceedings of the VCI2022 conference*, submitted to Nucl. Instrum. Meth. A.
- [2] H. Darwish et al., *Performance of the MIMOSIS-1 novel CMOS monolithic active pixel sensor, 23rd International Workshop on Radiation Imaging Detectors, Riva del Garda, Italy, 26–30 June 2022*.
- [3] CBM collaboration, Technical Design Report for the CBM Micro Vertex Detector (MVD), https://edms.cern.ch/ui/file/2738980/2/MVD_TDR_FINAL_Public.pdf (2021).
- [4] M. Al-Turany et al., *CBMRoot*, <https://git.cbm.gsi.de/computing/cbmroot>.
- [5] S. Agostinelli et al., *Geant4 — a simulation toolkit, Nucl. Instrum. Meth. A* **506** (2003) 250.
- [6] H. Darwish and M. Deveaux, *Heavy ions hits at the CBM-MVD*, CBM Progress Report 2020, <https://repository.gsi.de/record/237432/files/CBM%20Progress%20Report%202020.pdf>.
- [7] ALICE collaboration, H. Hillemanns, *Radiation Hardness of Monolithic Active Pixel Sensors and Readout Electronics for the ALICE Inner Tracking System Upgrade* https://indico.cern.ch/event/695271/contributions/2956083/attachments/1637991/2614211/CERN_LHC_Rad_symp_23042018_HHI.pdf (2018).

- [8] STAR collaboration, G. Contin, *The STAR PXL detector*, [2016 JINST 11 C12068](#).
- [9] CBM collaboration, *mCBM@SIS18*, <https://repository.gsi.de/record/220072> (2021).
- [10] JEDEC Solid State Technology Association, *Test procedures for the measurements of single-even effects in semiconductor devices from heavy ion irradiation*, *JESD57A* (1996), reaffirmed Sept. 2003.
- [11] J.F. Ziegler et al., *SRIM — the stopping and range of ions in matter*, *Nucl. Instrum. Meth. B* **268** (2010) 1818.

2023 JINST 18 C04002